Hines, B.R., Seebeck, H., Crampton, J.S., Bland, K.J., and Strogen, D.P., 2022, Reconstructing a dismembered Neogene basin along the active Hikurangi subduction margin, New Zealand: GSA Bulletin, https://doi.org/10.1130/B36308.1.

Supplemental Material

Text. Supplemental text.

Figure S1. Structural and physiographic features in the New Zealand region of the southwest Pacific.

Figure S2. Location of the eastern North Island in various pre-Miocene reconstructions of the proto-New Zealand subcontinent. Inset shows the outcome of the relative position of eastern North Island based on the dominant mode of deformation adopted by any particular reconstruction. Figure modified from King (2000) and Wood & Stagpoole (2007).

Figure S3. Major faults and structures discussed in text. Outcrop distributions of New Zealand's basement terranes, the Northland and East Coast allochthons, and the Taupō Volcanic Zone, are plotted for reference (see map legend).

Figure S4. Various assumptions about the orientation of the Dun Mountain-Maitai Terrane (and coincident Junction Magnetic Anomaly) and the Esk Head Belt during the late Eocene (45 Ma), along with predicted strikes for this time.

Figure S5. Block models for the ECB from previous studies, and this study.

Figure S6. Structural block divisions applied in the GPlates model of this study. Bounding structures and GPlates microplate code number as included in Table 1.

Figure S7. Different interpretations of late Neogene distribution of Te Aute Limestone lithofacies.

Figure S8. Burial history plots from selected representative sections and composite sections across the East Coast Basin.

Table S1. Additional declination anomaly data from various localities around New Zealand, not included in the Lamb (2011) paleomagnetic data compilation.

Table S2. Average strike orientation of basement and mid-Cretaceous strata in the North Island East Coast Basin. Strike and dip data extracted from QMAP 1:250,000 sheets (Begg & Johnston, 2000; Mazengarb & Speden, 2000; Lee & Begg, 2002; Lee *et al.*, 2011). Standard deviation (σ), number of observations (n).

1. INTRODUCTION

The propagation of the Australian-Pacific plate boundary through the New Zealand region in the late Eocene to early Miocene resulted in the development of a number of major physiographic features in the southwest Pacific region (Supplemental Figure S1). The position and geometry of the East Coast Basin prior to the inception of the modern plate boundary between the Australian and Pacific plates continues to be a contentious issue in paleogeographic reconstructions of the proto-New Zealand subcontinent (Zealandia; Mortimer et al., 2017) and the Southwest Pacific region (Supplemental Figure S2). The ultimate purpose of the structural model developed herein is to derive a palinspastic framework upon which the stratigraphic and paleoenvironmental development of the Late Cretaceous–Eocene East Coast Basin can be assessed. In order to produce a pre-Neogene model base, varied Neogene deformations must be sequentially back-stripped. Placing the East Coast Basin within a palinspastic model framework requires consideration of the structural trends of the wider New Zealand region. To do this, multiple geological and geophysical data sets are integrated to provide a holistic overview of regional and basin structural evolution during Neogene plate boundary propagation.

There is considerable variability in the location of the East Coast Basin in paleogeographic reconstructions of the southwest Pacific (Supplemental Figure S2; King, 2000). These reconstructions can be divided into two general schools of thought: one requiring considerable strike-slip movement and a minor rotational component (e.g., Cole, 1986; Ballance, 1976; Carter and Norris, 1976; Cooper and Tulloch, 1992; Beu, 1995); and the alternative, requiring substantial rotation of the region with a minor component of strike-slip displacement (e.g., Lamb, 1988; Gray and Norton, 1988; Uruski and Wood, 1993; Lewis and Pettinga, 1993; King, 2000; Nicol et al., 2007; Wood and Stagpoole, 2007; Seebeck et al., 2014). Considering that paleomagnetic studies have demonstrated that there has been 60–110° of Neogene vertical-axis rotation in the East Coast Basin (excluding the East Coast Allochthon; Mumme and Walcott, 1985; Mumme et al., 1989; Rowan and Roberts, 2008; Lamb, 2011), this would favor a reconstruction approach with a large rotational component and a comparatively minor strike-slip contribution. Such an interpretation is also supported by estimates of offset across major crustal-scale faults in North Island (e.g., Beanland et al., 1998; Nicol et al., 2007).

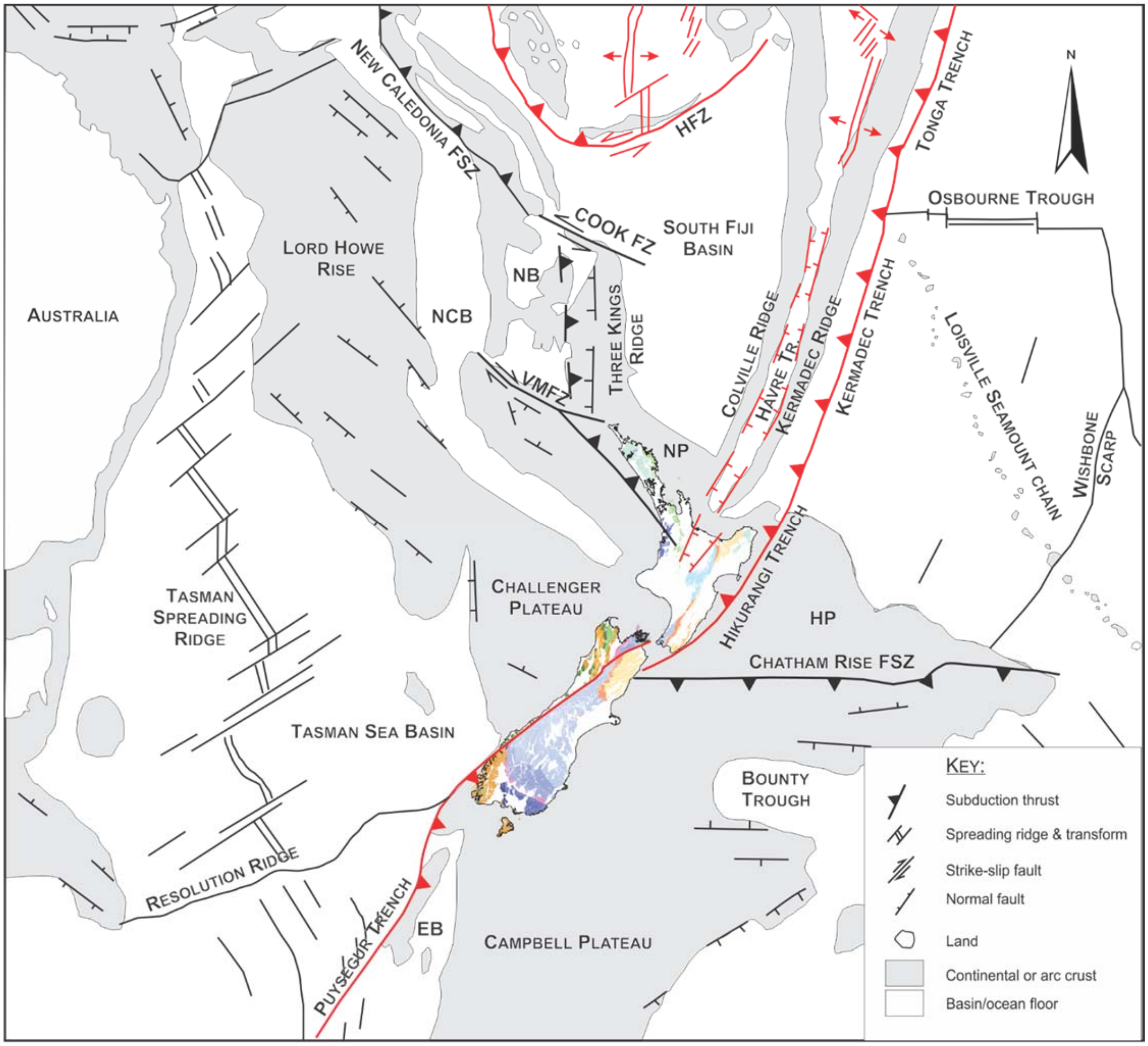

Supplemental Figure S1: Structural and physiographic features in the New Zealand region of the southwest Pacific. Key to abbreviations: HP – Hikurangi Plateau, EB - Emerald Basin, NP – Northland Plateau, NB – Norfolk Basin, NCB – New Caledonia Basin, VMFZ – Vening Meinesz fracture zone, HFZ – Hunter Fracture Zone, FSZ – Fossil Subduction Zone, FZ – fracture zone. Black denotes fossil and relict structures, red indicates active structures. Basement geology superimposed on New Zealand – see Supplemental Figure S3 for key. Onshore geology from Heron (2018), submarine physiographic and tectonic features from Schellart et al. (2006).

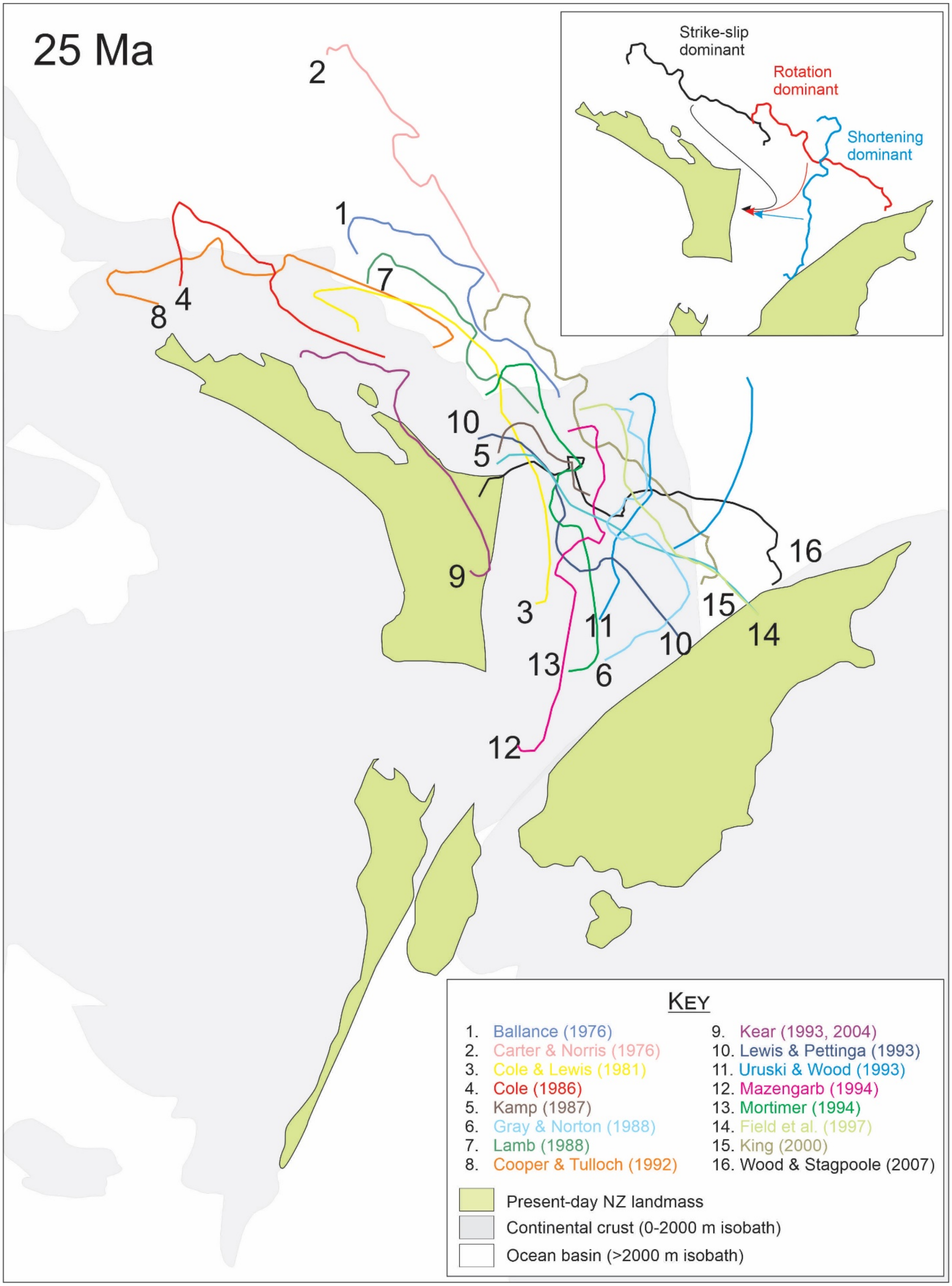
25 Ma
Strike-slip dominant
Rotation dominant
Shortening dominant
2
1
7
4
8
10
5
9
3
11
13
6
10
12
15
14
16
KEY
1. Ballance (1976)
2. Carter & Norris (1976)
3. Cole & Lewis (1981)
4. Cole (1986)
5. Kamp (1987)
6. Gray & Norton (1988)
7. Lamb (1988)
8. Cooper & Tulloch (1992)
9. Kear (1993, 2004)
10. Lewis & Pettinga (1993)
11. Uruski & Wood (1993)
12. Mazengarb (1994)
13. Mortimer (1994)
14. Field et al. (1997)
15. King (2000)
16. Wood & Stagpoole (2007)
Present-day NZ landmass
Continental crust (0-2000 m isobath)
Ocean basin (>2000 m isobath)

Supplemental Figure S2: Location of the eastern North Island in various pre-Miocene reconstructions of the proto-New Zealand subcontinent. Inset shows the outcome of the relative position of eastern North Island based on the dominant mode of deformation adopted by any particular reconstruction. Figure modified from King (2000) and Wood and Stagpoole (2007).

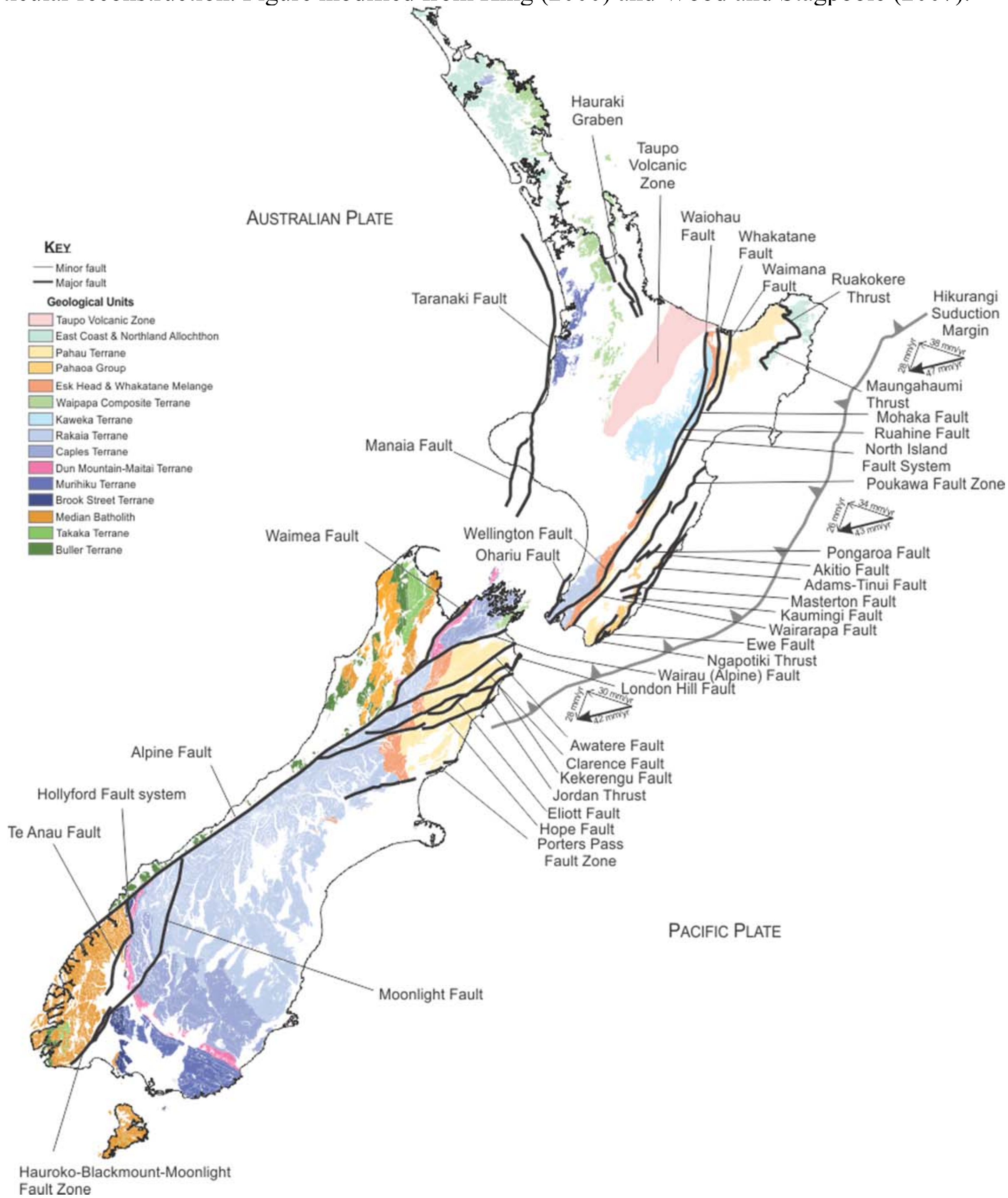

Supplemental Figure S3: Major faults and structures discussed in text. Outcrop distributions of New Zealand's basement terranes, the Northland and East Coast allochthons, and the Taupō

Volcanic Zone, are plotted for reference (see map legend). Map data sourced from Heron (2018). Relative plate motion vectors from Nicol et al. (2007).

2. TIMING AND NATURE OF OROCLINAL BENDING

Since the analysis of the Alpine Fault movement history by Harold Wellman in 1949 (in Benson, 1952), the timing and amount of bending of New Zealand basement terranes have been amongst the most debated topics in New Zealand geological literature (Kingma, 1959; Suggate, 1963; Wellman, 1971; Molnar et al., 1975; Carter and Norris, 1976; Walcott et al., 1981; Walcott, 1984; 1998; Kamp, 1987; Gray and Norton, 1988; Lamb and Bibby, 1989; Vickery and Lamb, 1995; Bradshaw et al., 1996; Little and Roberts, 1997; Sutherland, 1999a; King, 2000; Hall et al., 2004; Nicol et al., 2007; Lamb, 2011; Mortimer, 2014; Lamb et al., 2016).

Identification of basement piercing points is an important factor in resolving this debate. These include: Dun Mountain-Maitai Terrane, Esk Head Belt, axis of Haast Schist metamorphism, Mesozoic continental-ocean margin, Median Batholith, Darran Suite intrusives, regional syncline axes, Eocene rift margin (e.g., Sutherland et al., 2000), form-lines from steeply dipping-sub-vertical basement strata, and regional-scale Mesozoic faults in South Island (Mortimer, 2014; Lamb et al., 2016). On both sides of the Alpine Fault the trends of regional strike of basement rocks bend toward subparallel alignment with the Alpine Fault, defining an oroclinal bend (Wellman, 1956; King, 2000; Mortimer, 2014).

The Maitai Terrane includes the Dun Mountain ophiolite assemblage, which is associated closely with the Junction Magnetic Anomaly and gravity anomalies (Sutherland, 1999a, 1999b). The distinctive rock types and geophysical characteristics allow it to be mapped in detail across the country, providing a continental strain marker for deformation across Zealandia. Most models agree that the Dun Mountain-Maitai Terrane and coincident Junction Magnetic Anomaly was bent during the Mesozoic Rangitata Orogeny (Kamp, 1987; Bradshaw et al., 1996; Sutherland, 1999a). The debate has recently centered on whether the other major basement-derived structural lineation and piercing point, the Esk Head Belt, was bent in the Mesozoic or the Neogene (e.g., Mortimer, 2014; Lamb et al., 2016; van der Meer et al., 2016). Four possibilities for the pre-plate boundary development positions of the Dun Mountain-Maitai Terrane are considered (following Sutherland, 1999a):

(1a) Prior to 45 Ma, the Alpine Fault was a pre-existing structure that had already accumulated 350 km of sinistral offset (e.g., Lamb et al., 2016). This assumes a rigid plate motion model, with all relative displacement between the two plates being accommodated by slip on the Alpine Fault (Supplemental Figure S4).

(1b) The Alpine Fault existed prior to 45 Ma, but with <350 km of sinistral displacement, requiring most of the post-45 Ma displacement to be on the Alpine Fault, with a limited amount of distributed deformation (Supplemental Figure S4).

(2) The Alpine Fault formed after 45 Ma, with 480 km of dextral displacement, and 350 km of distributed shear across a zone adjacent to the Alpine Fault (e.g., Sutherland, 1999a; Cox and Sutherland, 2007; Supplemental Figure S4).

(3) Prior to 45 Ma, the Alpine Fault existed with <480 km of dextral offset, requiring a substantial proportion of plate boundary offset since 45 Ma to be distributed as crustal deformation west of the Alpine Fault (e.g., van der Meer et al., 2016; Supplemental Figure S4).

Contemporary strain measurements and paleomagnetic data demonstrate that there has been a component of distributed dextral shear across the Cenozoic plate boundary (Walcott, 1984; Lamb, 2011; Little and Roberts, 1997; Sutherland, 1999a), including high Cenozoic brittle strain within 100 km of the Alpine Fault that has resulted in the Murihiku Terrane being dispersed as fault slivers (Mortimer, 2014). If there was dextral strike-slip prior to 45 Ma, then a complex S-shaped geometry must be required (Supplemental Figure S4), with a large proportion of plate motion since 45 Ma distributed as continental deformation, rather than being focused on the Alpine Fault, as the total plate motion is well-constrained (Sutherland, 1999a). This leaves two primary hypotheses for the development of the oroclinal bend through New Zealand, which have largely divided models and reconstructions into two camps, with much debate.

Kamp (1987) and Sutherland (1999a) suggest that the Dun Mountain-Maitai Terrane was modestly deformed to create a smooth, continuously curved geometry during the late Triassic accretion of the Rakaia Terrane, implying that most deformation occurred during the late Oligocene–Neogene (Supplemental Figure S4b). This suggests that of the ~780 km of post-Eocene relative movement between the Australian and Pacific plates, >50% (480 km) has been partitioned into the Alpine Fault, and the remainder accommodated by distributed shear, mainly within the Southern Alps (Sutherland, 1999a; Sutherland et al., 2000; Cox and Sutherland, 2007). Subsequently, the Dun Mountain-Maitai Terrane was additionally deformed, and the Esk Head Belt primarily deformed during Neogene deformation. The alternative model implies pre-Eocene, likely Cretaceous sinistral movement of the Alpine Fault, which is then reactivated in the Neogene with a substantial dextral displacement (e.g., Lamb et al., 2016). There are compelling arguments for mid-Cretaceous bending of the Gondwana continental margin at c. 105 Ma, associated with the collision of the Hikurangi Plateau with the Mesozoic subduction system (e.g., Davy et al., 2008; Reyners et al., 2011, 2017; Crampton et al., 2019; Supplemental Figure S4c).

A largely Neogene origin for the development of oroclinal bending is adopted in the model presented here (Supplemental Figure S4b). The Esk Head Belt (170 Ma; Adams et al., 2011) is a substantially younger feature than Dun Mountain-Maitai Terrane (280 Ma; Kimborough et al., 1992), providing 110 Myr to deform the Dun Mountain-Maitai Terrane before the accretion of the Esk Head Belt. This aside, there is no requirement for orogenic belts to form linear features over large distances (e.g., the orogenic belt associated with the Talaud Orogeny, North Moluccas, Indonesia; Simandjuntak and Barber, 1996); and it is certainly possible that the Esk Head Belt originated with some degree of bending. Irrespective of this, rigid plate reconstruction of this strain marker across the Alpine-Wairau Fault can be achieved in ~4.5 Myrs at full (current) relative plate motion rates, which suggests the ~150 km offset presently observed has accrued since the middle Miocene. The rotation and translation of a number of the basement markers and piercing points can be explained by simple post-Eocene rigid rotation and translation of the Australian Plate relative to the Pacific Plate as the Emerald Basin opened (Sutherland, 1995; Mortimer, 2014). There is evidence of large-scale, Neogene deformation in the Emerald Basin that would support Neogene bending of the orocline (Hayes et al., 2009). Additionally, there is evidence of tightening of the Southland Syncline concurrent with post-Oligocene oroclinal bending (Little and Mortimer, 2001).

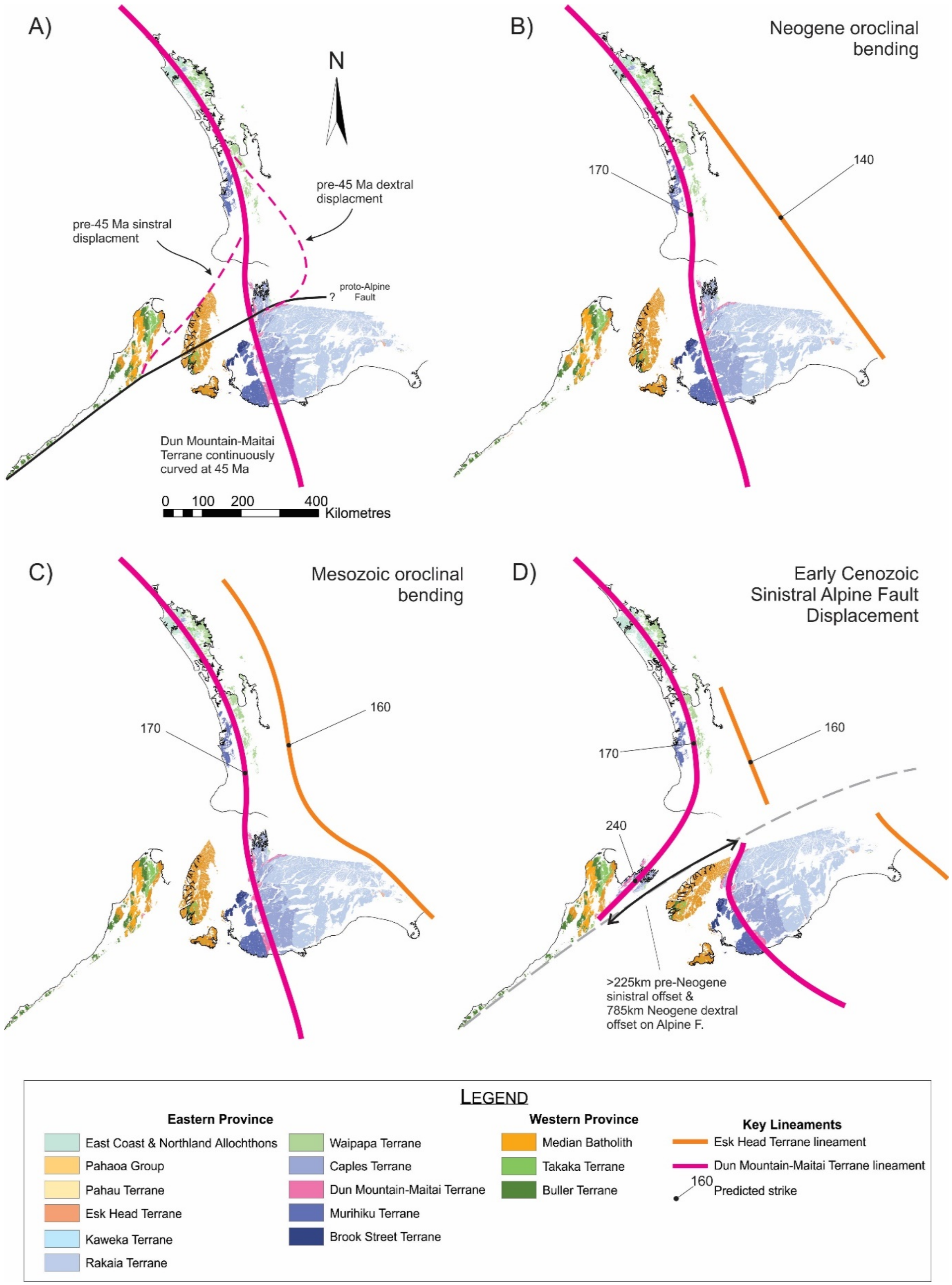

Supplemental Figure S4: Various assumptions about the orientation of the Dun Mountain-Maitai Terrane (and coincident Junction Magnetic Anomaly) and the Esk Head Belt during the late

Eocene (45 Ma), along with predicted strikes for this time. A) Geometry for a continuously curved, both dextrally and sinistrally displaced Dun Mountain-Maitai Terrane at 45 Ma (modified after Sutherland, 1999a). B) Geometry of the Esk Head Belt assuming dominantly Neogene oroclinal bending. This model is adopted in this study. C) Geometry for the Esk Head Belt adopting Mesozoic oroclinal bending. D) Geometry of the Dun Mountain-Maitai Terrane and Esk Head Belt for pre-Neogene sinistral displacement on the Alpine Fault (Lamb et al., 2016). The East Coast and Marlborough outcrop geology has been omitted for clarity. Broad regional structural divisions displayed here are representative of the King (2000) crustal blocks.

3. BLOCK MODEL DEVELOPMENT

3.1 Block Assignment and Definition

Of the assumptions required in order to establish the baseline for the model, arguably the most important is the definition of continental blocks, and determining the precursor relationships between these continental blocks (King, 2000). Block boundaries applied herein are defined primarily on the basis of geological and structural considerations, and also changes in gravity and magnetic data. Preference for structural division was given to faults that demonstrated evidence of early Miocene or pre-Neogene existence, and structures that form distinctive features within the geological, structural and physiographical division of the New Zealand region. In most cases, block divisions are well-defined by discrete structures, although in a few places block boundaries are considered a diffuse zone of faulting and deformation. The division of structural blocks along basement-penetrating faults of Early or pre-Miocene age, with consideration of pre-Neogene geology, has resulted in a similar structural subdivision of the North Island East Coast to that of Moore (1988; Supplemental Figure S5a). Although the model presented here draws on previous GPS-based models (e.g., Wallace et al., 2004, 2012; Supplemental Figure S5b) and paleomagnetism-based reconstructions (e.g., Lamb, 2011; Supplemental Figure S5c), block geometries applied here in this study differ substantially from previous reconstructions (Supplemental Figure S5d). These structural subdivisions have been simplified for expression within the model, with often moderately complex geometries reduced to simple block structures and straight boundaries for clarity of presentation. In the present-day offshore region, the blocks are limited by the 2000 m isobath. In establishing the base model, the wider Zealandia region is divided into five major crustal blocks, following King (2000), but with further subdivision in the Taranaki, Marlborough and East Coast areas. In this model, the East Coast Basin (ECB) is represented by a number of separate crustal blocks that move independently within a basin-scale envelope.

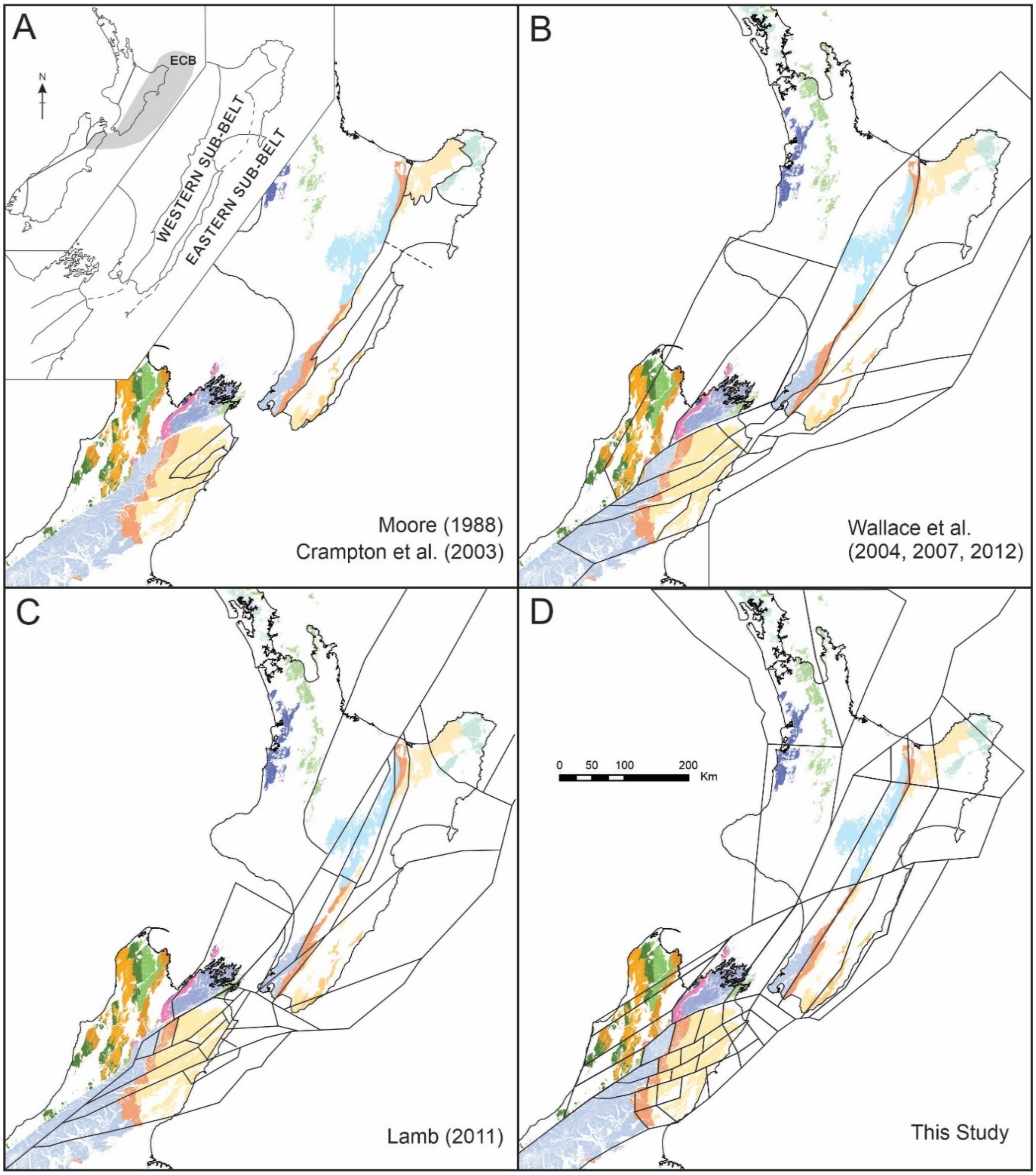

Supplemental Figure S5: Block models for the ECB from previous studies, and this study. A) North Island structural divisions from Moore (1988), and South Island block divisions from Crampton et al. (2003). Sub-belts shown for reference from Moore (1988, modified after Crampton, 1997). New Zealand broad-scale block divisions of King (2000) shown in inset map. B) Block model from Wallace et al. (2004, 2007, 2012) for Pliocene movements of the ECB. C) Neogene model from Lamb (2011). D) The structural block divisions adopted in this study.

3.2 East Coast Structural Division

In the model developed and presented herein, the North Island ECB has been simplified along major structural trends and tectono-geomorphic features. Subdividing the basin along major, crustal-scale and basement-penetrating structures has essentially produced a micro-plate model for the East Coast region that is detailed enough so that aspects of brittle deformation, particularly strike-slip motions, are not obscured, but without getting lost in minute, obscured and largely unresolved variability across the basin (Fig. 2; Supplemental Figure S5). Similarly, such a division allows the paleomagnetic histories of individual fault-bounded blocks to be incorporated into the reconstructions.

Within the ECB, blocks have been divided along structures that have demonstrated significant vertical or horizontal displacement, with a preference for faults displacing pre-Neogene strata. The ECB has been simplified along major structural trends and tectono-geomorphic features. In the North Island, structural blocks were formed by subdividing the basin along major, crustal-scale and basement-penetrating structures of the North Island Fault System (Beanland et al., 1998; Nicol et al., 2007; Bland et al., 2019), notably the Ohariu Fault, Wellington and Wairarapa faults and the corresponding Mohaka and Ruahine faults; the Whakatane Fault, Waiohau Fault, and Waimana Fault. Major block-bounding structures are summarized in Table 1.

The East Coast Allochthon/Raukumara structural block (22) is delineated by the Ruakokere and Maungahaumi thrusts (following Mazengarb and Harris (1994) and Leonard et al. (2010)). The southern boundary of this block is largely inferred, due to the absence of pre-Neogene outcrop or notable structures, and late Neogene sedimentary strata obscuring structural boundaries (Moore, 1988; Mazengarb and Harris, 1994). The North Island axial ranges are divided into two separate blocks, namely the Urewera Range (20) and the Ruahine-Tararua-Rimutaka ranges (15; Supplemental Figure S6). West of the axial ranges, the Kaimanawa Mountains (27) and Kapiti Island (14) have been differentiated from the axial ranges on the basis of higher metamorphic grade in basement strata. The Kaimanawa block (27) is delineated by the Ngamatea Fault in the east, and the Taupō Volcanic Zone (TVZ) to the west, and basement strata are comprised, in part, of Kaimanawa Schist (Mortimer, 1993). The Kapiti block (13) is differentiated by a change in basement strata composition (Waipapa Terrane) and metamorphic zonation across the Ohariu Fault that can be correlated with low grade schist in the Marlborough Sounds (Mortimer, 1993; Adams and Graham, 1996; Adams et al., 2009). East of the axial ranges, the Raukumara Ranges (23) and northern Urewera Ranges (25) have been differentiated along the Whakatane Fault. South of this, the modern forearc basin is subdivided into a Hawke's Bay block (18) and a Wairarapa block (16), separated from the axial ranges by the Wellington-Ruahine-Mohaka fault system (Supplemental Figure S6; Table 1). The outer forearc-coastal ranges are again separated into separate Hawke's Bay (28) and Wairarapa (17) structural blocks, delineated as continuous linear feature by splays and relay structures between the Wairarapa, Alfredton, Matuki, Tukituki and Poukawa fault zones (Supplemental Figure S6; Table 1). There are limited offshore data available across Hawke Bay, although the trend of the Napier Fault, Pania Reef and the Cretaceous stratigraphy of the Opoutama-1 well on Mahia Peninsula provide a guide for the placement of this boundary (Mazengarb and Speden, 2000; Lee et al., 2011). Offshore, the accretionary prism is treated as a single structural block (29), following Wallace et al. (2004).

The Cook Strait area is divided into a complex series of en-echelon-style fault blocks (Pondard and Barnes, 2010; Holdgate and Grapes, 2015), which have been simplified within the broader context of our model. Importantly, the Cook Strait area marks the transition from continent-ocean subduction in the accretionary prism, into continental-continental transpressional tectonics in Marlborough.

Marlborough has been divided across the major structures of the Marlborough Fault System (Wairau, Awatere, Clarence, London Hill, Fidget, Jordan Thrust, Kekerengu, and Porters Pass faults), and further divided across smaller, obliquely oriented shear zones within the larger structures. Particularly for northern Marlborough, the division and reorganisation of the crust into smaller, equidimensional blocks is more representative of vertical-axis rotation and late Neogene deformation (Hall et al., 2004). The approximately equidistant subdivision of structural blocks in Marlborough allows correlation of key piercing points, in particular the Esk Head Belt, allowing rotation and correlation of Marlborough structural blocks with their North Island counterparts, without creating an unrealistic, splayed fan-like continental margin in reconstructions (an issue encountered in early iterations of this modeling approach).

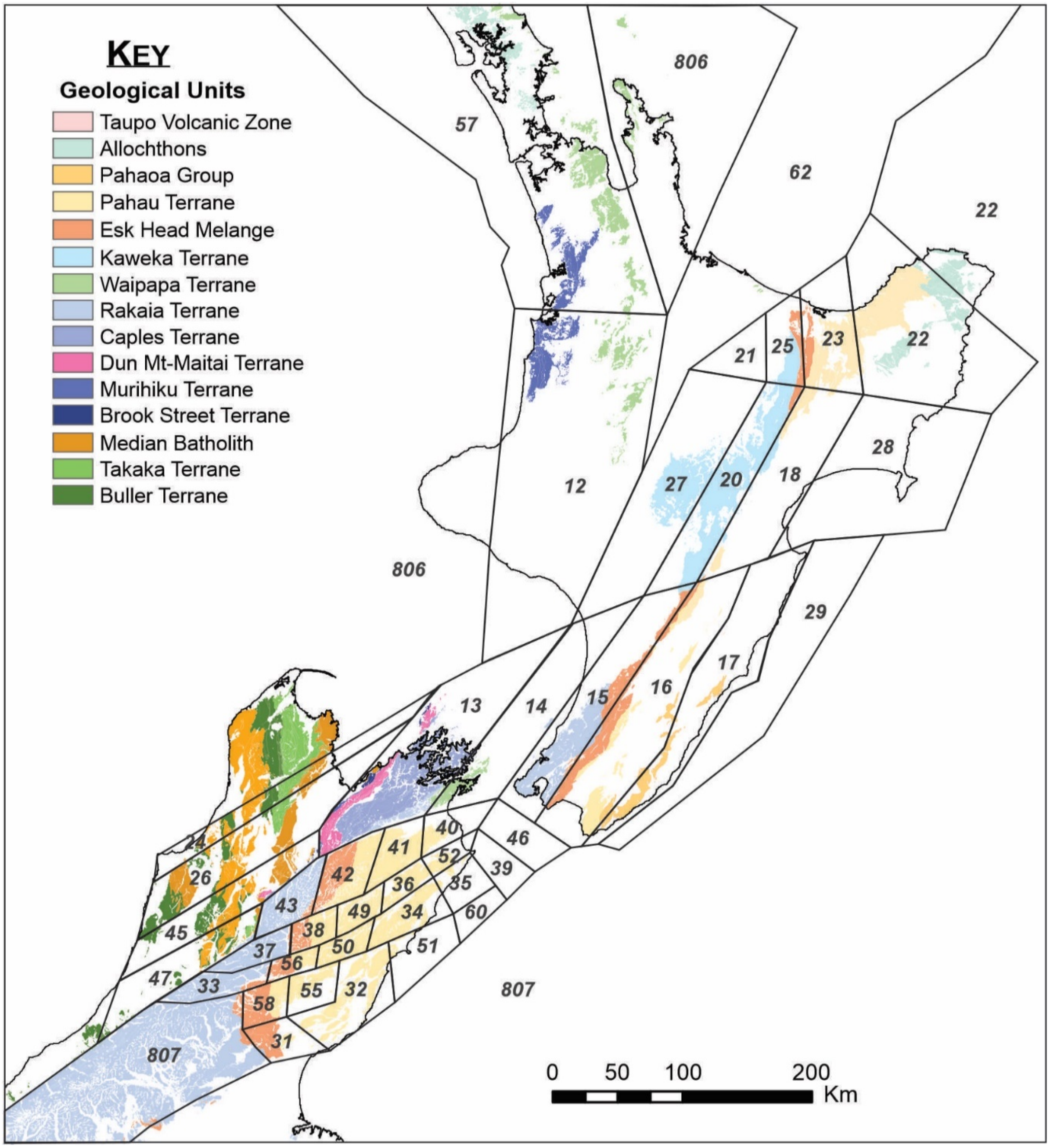

Supplemental Figure S6: Structural block divisions applied in the GPlates model of this study. Bounding structures and GPlates microplate code number as included in Table 1. Spatial distributions of New Zealand's basement terranes, the Northland and East Coast allochthons, and the Taupō Volcanic Zone, are plotted for reference (see map legend). Map data sourced from Heron (2018).

3.3 Strike-Slip Movements

Strike-slip estimates on specific structures compiled for this report are presented in Table 2, and discussed in further detail below. Faults in the North Island do not appear to have exceeded ~20 km of total strike-slip displacement individually, and strike-slip displacements of more than a few kilometres cannot be reliably demonstrated on any faults in the North Island Fault System (Nicol et al., 2007). During the late Neogene, there has been minimal strike-slip motion on NE–SW-oriented fault systems, with most displacement occurring during the Plio-Pleistocene (Cashman et al., 1992; Erdman and Kelsey 1992; Beanland et al., 1998; Nicol et al., 2007; Nicol and Wallace, 2007; Bland et al., 2019).

The Mohaka and Ruahine faults lack appropriate markers for the determination of net horizontal displacement (Erdman and Kelsey, 1992). However, estimates derived from late Neogene sedimentary rocks suggest that dextral strike-slip across the Ruahine Fault since the early Pliocene is likely to be less than 10 km, and the Mohaka Fault has had <2 km of strike-slip displacement since 2 Ma (Beanland et al., 1998; Bland and Kamp, 2006). Nicol et al. (2007) and Bland et al. (2019) suggest a maximum displacement across the Wellington-Mohaka fault system of ~20 km in the last 2.4–3.7 Myr.

A displacement of 16–22 km of dextral displacement is estimated across the Poukawa Fault Zone since the Late Pliocene, based on a re-alignment of outcropping ridges of mid-Pliocene Awapapa Limestone (Cashman et al., 1992). In the retro-deformation along the Poukawa Fault Zone presented by Cashman et al. (1992), alignment of the fault displaced positions of the Awapapa Limestone also require ~25° of anticlockwise rotation since c. 3.5 Ma, consistent with the vertical-axis rotation trends demonstrated in paleomagnetic data at this time (Fig. 3).

The Pongaroa-Waihoki Fault Zone has been active since the Otaian (21.7–18.7 Ma), with ~13 km of dextral strike-slip displacement on the Pongaroa Fault during the Early to Middle Miocene (Ridd, 1967). Northeast-trending faults along the Coastal Ranges (e.g., the Adams-Tinui Fault) have been suggested to have accommodated ~300 km of Neogene transcurrent movement (e.g., Delteil et al., 1996). This implied displacement is unreasonable in the context of geological constraints, especially given the narrow, 3 Myr window that this strike-slip displacement is inferred to have occurred. Minimal lateral movement along the Adams-Tinui Fault is interpreted in this model, consistent with Moore (1988).

The Wellington Fault at Te Marua shows 8 km of dextral strike separation and distributed shear across the Esk Head Belt, comparable with 7 ± 1 km displacements of major rivers across the Wellington Fault (Berryman et al., 2002; Nicol et al., 2007). The total strike-slip on the Wellington Fault is comparable with the estimated lateral displacement on the Ruahine and Mohaka Fault systems (Nicol et al., 2007; Bland et al., 2019).

The distribution of the Te Aute lithofacies limestones (Supplemental Figure S7a) have been revised herein to demonstrate that late Neogene strike-slip motion on the Wairarapa, Alfredton, Mangatarata, Tukituki and Poukawa fault zones is on the order of distribution of these fault systems shows that this estimate can be significantly reduced. The linear distribution of the Te Aute lithofacies is much more geologically reasonable (Supplemental Figure S7b), consistent with a long seaway through the region at this time (e.g., Trewick and Bland, 2012), and produces strike-slip estimates comparable to other indicators of strike-slip in the basin.

The Esk Head Belt demonstrates dextral displacement across the Wairau, Awatere, Clarence, and Hope Faults (Silberling et al., 1988; Hall et al., 2004; Lamb, 2011; Mortimer, 2014). Within the Marlborough Fault System, the Esk Head Belt has an aggregated dextral offset of 55 km, and across the Wairau-Alpine Fault and Cook Strait, the Esk Head Belt is offset by 150 km (Begg and Johnston, 2000; Rattenbury et al., 2006; Forsyth et al., 2008; Mortimer, 2014).

Within the Marlborough Fault System, Little and Jones (1998) demonstrate that the Awatere Fault system has only been active since c. 7 Ma, during which time it has accrued 34 km of dextral strike-slip motion. Crampton et al. (2003) estimate 25 ± 10 km of strike-slip across the Clarence Fault based on the present-day distribution of the Late Cretaceous Warder Coal Measures. Similarly, strike-slip displacement of 16–35 km on the Clarence Fault would bring the thickest sections of the Late Cretaceous extrusive Gridiron Volcanics to a point adjacent to the correlative intrusive, the Tapuae-O-Ueneku Igneous Complex (Crampton et al., 2003). Strike-slip displacement on the Jordan Thrust and the Kekerengu Fault is estimated to be ~5 km (Van Dissen, 1989; Van Dissen and Yeates, 1991; Crampton et al., 2003), although Quaternary fault slip data suggests that as much as 15 km of strike-slip movement may have been transferred from the Hope Fault onto the Kekerengu Fault and Jordan Thrust (Crampton et al., 2003). Dextral displacement on the Hope Fault is estimated to be 20 km based on the offset of conglomerate beds within the Torlesse (Freund, 1971; Crampton et al., 2003). Evidence, including syn-sedimentary deformation within the Great Marlborough Conglomerate, suggest that during the Early Miocene, a proto-Marlborough Fault System linked the early Hikurangi subduction system with the proto-Alpine Fault across the newly-formed plate boundary (Lamb and Bibby, 1989; Little and Jones, 1998). Through most of the Miocene, plate motion through South Island and across the Marlborough Fault System was slightly divergent or pure strike-slip, becoming slightly convergent after ~12 Ma, with increased convergence after 6.4 Ma following a southwest shift in Euler pole position (Walcott, 1998; Sutherland, 1995; Little and Jones, 1998). Initiation of significant strike-slip movement on the Marlborough Fault System is well-constrained between 6.4 and 7.4 Ma (Little and Jones, 1998).

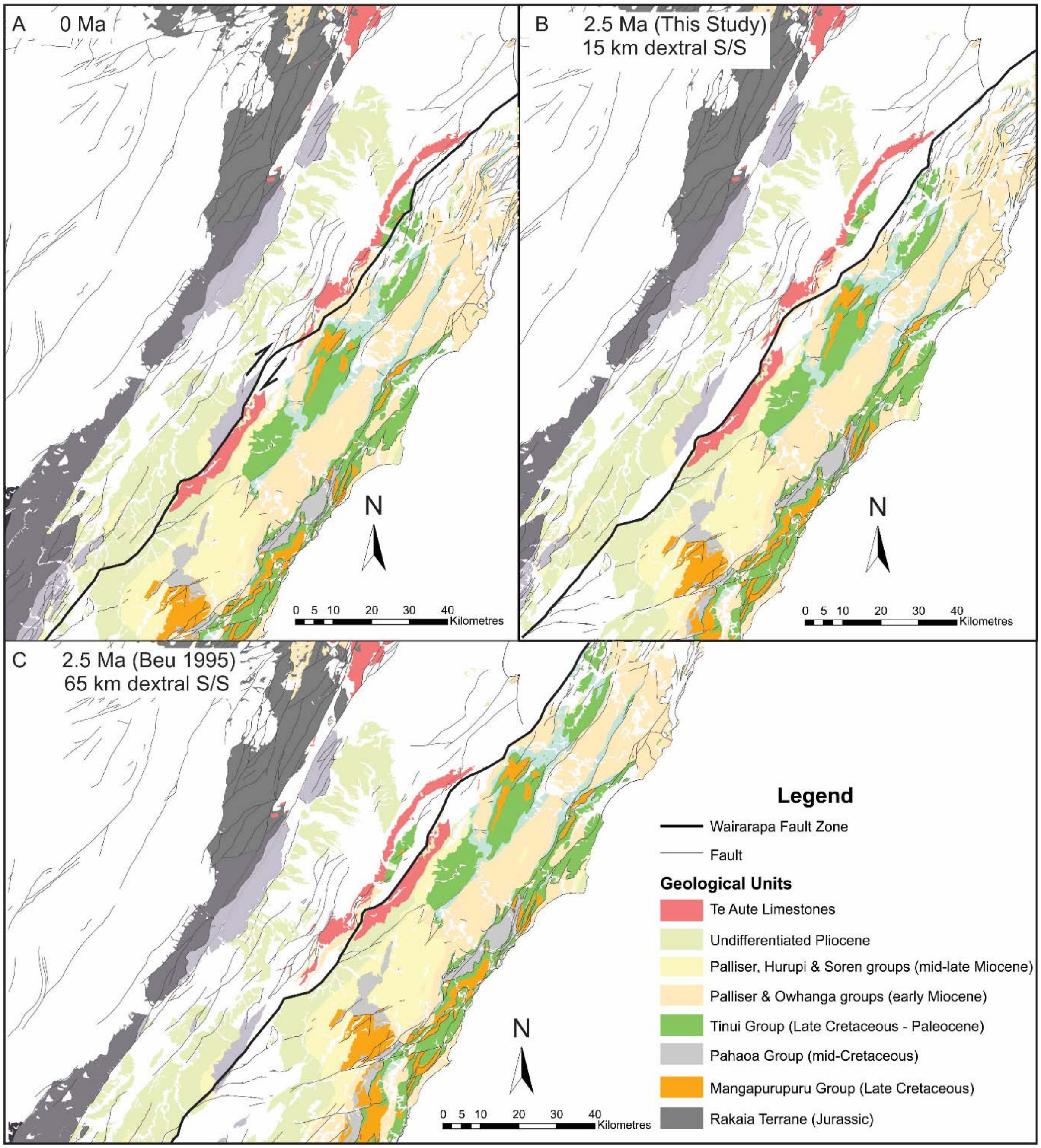

Supplemental Figure S7: Different interpretations of late Neogene distribution of Te Aute Limestone lithofacies. A) Present-day distribution of the Te Aute lithofacies limestones. B) Retro-deformation for the Mangapanian Stage (2.4 – 3.0 Ma) adopted by this study, resulting in ~15 km of strike-slip displacement distributed across the Wairarapa, Alfredton, Mangatarata, Tukituki and Poukawa fault zones. C) Reconstruction of the Mangapanian Stage from Beu (1995), with 65 km of strike-slip movement distributed across the same fault systems, resulting in a very different outcrop distribution of Te Aute lithofacies limestones. Map data sourced from Heron (2018).

3.4 Shortening

Neogene shortening, in the context of the model presented herein, is dominantly within the ECB. To reconstruct spatial relationships of structural blocks through time, it is necessary to estimate the amount, timing, location and orientation of shortening on significant structures in the ECB. Results of this analysis are summarized in Table 3. The tectonic regime has been dominated by shortening since the initiation of subduction in the Early Miocene (Field and Uruski, 1997), interrupted by at least two tectonic reorganisations since the Late Miocene. Most of the Neogene convergent plate motion in eastern North Island has been accommodated on the subduction interface (Nicol et al., 2007). Average shortening rates of 3–8 mm/yr in the upper plate are much lower than the average of 34 mm/yr rate of plate convergence since the Oligocene, making the subduction interface the most important contractional structure in the North Island (Nicol et al. 2007). Development of the Hikurangi Margin included early Miocene shortening of ~90 km (50 km across the ECB, and 40 km across the axial ranges), and not in excess of 150 km (Nicol et al., 2007). Section construction and restoration results in an estimated ~56 km of cumulative shortening across northern Marlborough, with estimates decreasing southwards (Crampton et al., 2003). The location and magnitude of shortening vary spatially across the Marlborough region and estimates are summarized in Table 3.

Early Miocene thrusting is interpreted to have occurred along the length of the Hikurangi Margin, suggesting that subduction reached its southernmost extent at or prior to 18 Ma (Chanier and Férriere, 1989; Rait et al., 1991; Delteil et al., 1996; Nicol et al., 2007). The Early Miocene thrusting episode responsible for the stacking of thrust sheets in the Raukumara Peninsula and Wairarapa had a 6–7 Myr duration (Chanier and Ferriere, 1991). Periods of accelerated deformation occurred during the Middle and Late Miocene (11–14 Ma and 5–7 Ma) (Field and Uruski, 1997; Chanier et al., 1999; Kamp, 1999; Nicol et al., 2002). Shortening occurred dominantly adjacent to the axial ranges, in a 20–50 km wide zone immediately east of the ranges, and in the ~50 km immediately adjacent to the subduction margin (Nicol et al., 2007). The upper flanks of the Ruahine and Kaweka ranges have in places marine rocks c. 2.4 Ma in age, although uplift of the ranges is interpreted to both predate and postdate deposition of these strata (Nicol et al., 2007). This is in line with two phases of uplift proposed for the axial ranges since 5 Ma; after ~1.5 Ma and 2.5–3.7 Ma (Melhuish, 1990; Beanland et al., 1998; Nicol et al., 2007).

3.5 Extension

There is very little evidence for Neogene extension in the ECB, although extension associated with thrust complexes within the accretionary prism in Hawke Bay during the Middle to Late Miocene (c. 14–4 Ma) has been noted by Barnes and Nicol (2004), Nicol and Uruski (2005) and Burgreen-Chan et al. (2016). These formed through polyphase deformation on an opposed dipping thrust duplex under a compressional regime (Barnes and Nicol, 2004). Uruski (1992) identified several sub-basins in Cook Strait that initially developed as half-grabens resulting from Late Cretaceous to Paleocene rifting, before developing into pull-apart basins in the Neogene due to transcurrent faulting in Marlborough and the North Island.

3.6 Reactivated Structures

The Neogene structural division of the New Zealand region (excluding the TVZ) appears to be largely governed by existing, mostly Cretaceous-aged structures. The Alpine Fault formed through the growth and interconnection of smaller faults as displacement of the boundary increased, until reaching the present-day length of 600 km; i.e., a zone of faults that became progressively interconnected during Miocene times (Sutherland, 1999a). Therefore, the Alpine Fault as a continuous structure may be much younger than the Oligocene to early Miocene age generally accepted for its inception (Sutherland, 1999a). Alternatively, the Alpine Fault was an existing Cretaceous structure that already had hundreds of kilometres of sinistral offset prior to the Neogene (Lamb et al., 2016). Several major faults in the ECB were active structures in the Late Cretaceous (Nicol et al., 2007; Stagpoole and Nicol, 2008; Crampton et al., 1998). These include the Mohaka Fault, the Adams-Tinui Fault and the Clarence Fault (Moore, 1980; Crampton and Moore, 1990; Isaac et al., 1991; Crampton et al., 2003).

Several major faults in North Island were active structures in the Late Cretaceous (Nicol et al., 2007; Stagpoole and Nicol, 2008; Reilly et al., 2015; Crampton et al., 1998). These include the Mohaka Fault, for which there must have been an earlier, Cretaceous structure prior to the Campanian-Maastrichtian (Piripauan – Haumurian), as Pahau Terrane is juxtaposed against Late Cretaceous Karekare Formation, both of which are demonstrably overlain by Campanian-Maastrichtian (Piripauan–Haumurian) Tahora Formation (Crampton and Moore, 1990; Isaac et al., 1991). The Adams-Tinui Fault was interpreted as an active structure in the latest Cretaceous by Moore (1980).

4. GEOHISTORY MODEL DEVELOPMENT

Construction of burial history plots (Supplemental Figure S8) follows the method of Bland et al. (2019), where GNS Science's spreadsheet-based Geohistory tool was applied, producing a model that allows for variable sedimentation rates and sediment compaction. Unit thickness imputed into the tool are decompacted by formation in accordance with Sclater and Christie (1980) and plotted as total sediment thickness through time. Decompaction utilizes the simple exponential approach of Athy (1930) and generalized lithologic compositions for deposited units with compaction parameters based on data from the nearby Taranaki Basin (Armstrong et al., 1996). Unconformities are inserted as missing section. Estimates of missing section are derived from the thickness of stratigraphic intervals in adjacent regions and/or from estimates of eroded section derived from bulk density analyses of mudstone strata (e.g., Kamp et al., 2004; Pulford and Stern 2004). The ages of unconformities are constrained by ages of units separated by the unconformity. The sedimentation rate for missing section is normally matched to rates for the underlying unit, allowing appropriate time for uplift. Dashed lines are used to represent the poorly constrained burial history related to the commonly eroded section of the Quaternary Period. Geological and geochronological data are sourced from detailed measured sections compiled during the East Coast Cretaceous-Cenozoic program (Field and Uruski, 1997), with the most complete or representative sections used from each region presented. Burial history plots for the Tawhero Basin and Te Muna area were compiled using data sourced from Neef (1997) and Nicol et al. (2002) respectively. Paleowater depth estimates are determined through the application of benthic foraminiferal and molluscan macrofaunal data sets.

Burial history plots indicate a small amount of shortening in the Tawhero Basin from 18 to 10 Ma, before basin subsidence accelerated at 8–9 Ma. Basin subsidence initiated in the Hawkes Bay at 11–12Ma (Mohaka River and Hawkes Bay composite section). The acceleration of basin subsidence is broadly consistent across the ECB, occurring at ~9–10 Ma in the Hawkes Bay (Mohaka and Hawkes Bay composite sections), Wairarapa (Te Muna and Tawhero sections) and Marlborough region (north Marlborough composite section). Shortening in the Marlborough region begins at 10–8 Ma, consistent with the timing of the propagation of the Wairau Fault and development of the Marlborough Fault System. Basin subsidence at Tutaekuri River initiates at 8–9 Ma, reaching a peak at 2–2.5 Ma, consistent with a rapid basin subsidence recognized in the Kereru-1 borehole (Bland et al., 2019). Basin subsidence in the southern Wairarapa is initiated at ~11 Ma.

Throughout the Hawke's Bay, Wairarapa and Marlborough regions there are recuring intervals of terrestrial conglomerate deposition bracketed by deep-marine sediments, providing strong geological evidence for the timing of significant vertical motions in the ECB. These events are constrained to three distinct periods: 18–16 Ma (e.g., Takiritini Formation; Neef, 1997), 11–9 Ma (e.g., Putangirua, Mangaoranga, Ngarata, Sunnyside and Medway formations; Neef, 1997; Nicol et al., 2002; Bland et al., 2007; Wells, 1989; Kelsey et al., 1995; Browne, 1995; Bertaud-Gandar et al., 2018), and 6–5 Ma events (e.g., Blowhard, Mangahururu, upper Medway and Upton formations; Browne, 1995, 2004; Bland et al., 2007; Cutten, 1988). These conglomerates are inferred to mark times of accelerated uplift and erosion of geological basement rocks, together with the uplift of deep-marine environments to terrestrial settings. The inference is that the uplift is driven by accelerated crustal shortening.

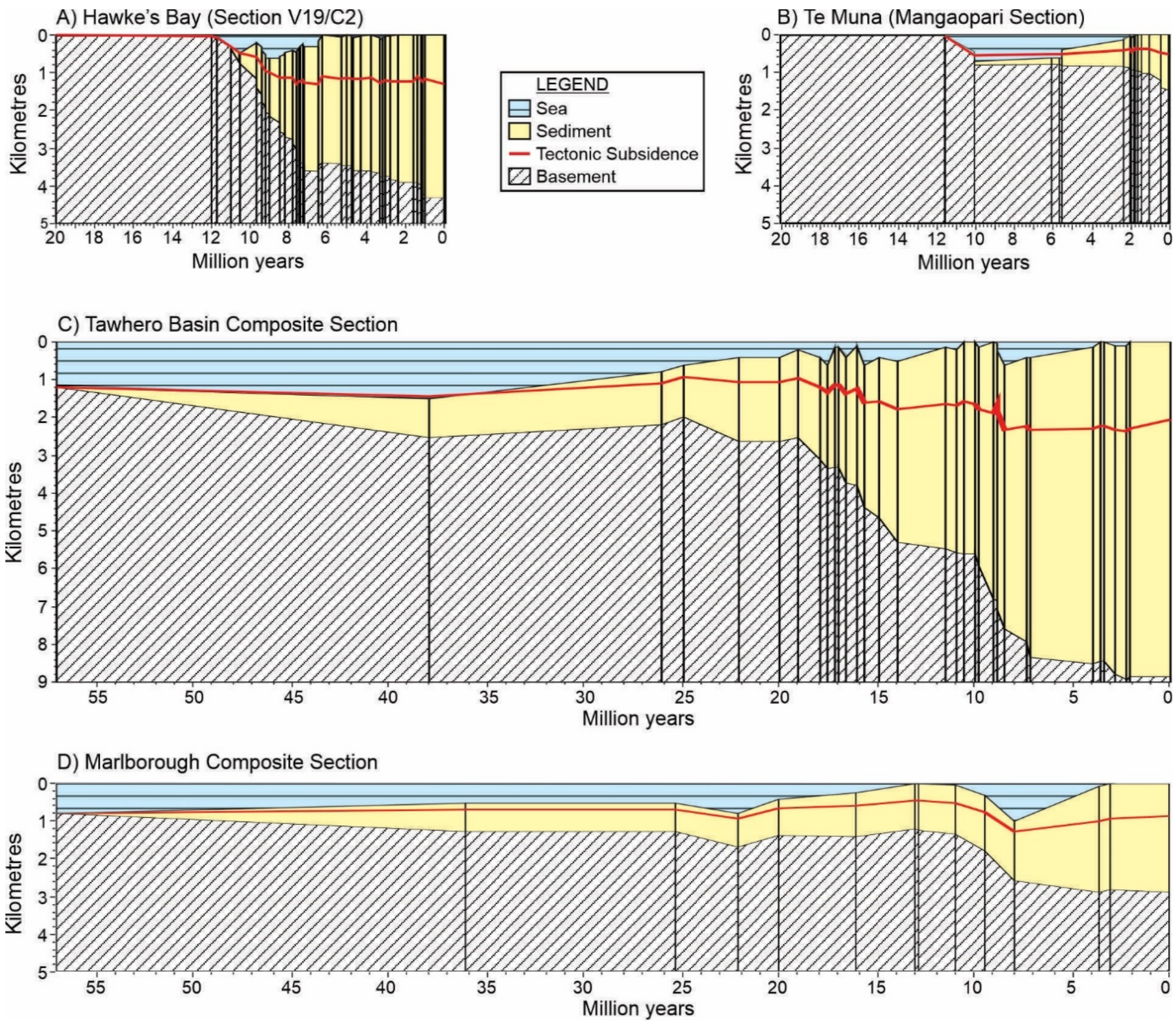

Supplemental Figure S8: Burial history plots from selected representative sections and composite sections across the East Coast Basin. Plots were constructed using GNS Science's 'Geohistory' spreadsheet-based software tool. Models include estimates of sediment compaction derived from generalized lithological compositions of units. Paleowater depth estimates are determined from benthic foraminiferal and molluscan assemblages. Input data for Model A (Hawke's Bay [Section V19/C2]) are primarily sourced from Field and Uruski (1997). Input data for Model B (Te Muna [Mangaopari section], southern Wairarapa) sourced from Bertaud-Gandar et al., 2018; Field et al., 1997; Nicol et al., 2002). Input for Model C (Tawhero Basin composite section, northeast Wairarapa), compiled from Neef (1997) and Field and Uruski (1997). Input data from Model D (central-northern Marlborough composite section), primarily compiled from Browne (1995) and Field and Uruski (1997).

REFERENCES CITED

Adams, C., and Graham, I., 1996, Metamorphic and tectonic geochronology of the Torlesse terrane, Wellington, New Zealand: New Zealand Journal of Geology and Geophysics, v. 39, no. 2, p. 157–180, https://doi.org/10.1080/00288306.1996.9514703.

Adams, C., Mortimer, N., Campbell, H., and Griffin, W., 2011, Recognition of the Kaweka Terrane in northern South Island, New Zealand: preliminary evidence from Rb–Sr metamorphic and U–Pb detrital zircon ages: New Zealand Journal of Geology and Geophysics, v. 54, no. 3, p. 291–309, https://doi.org/10.1080/00288306.2011.569728.

Adams, C., Mortimer, N., Campbell, H., and Griffin, W.L., 2009, Age and isotopic characterisation of metasedimentary rocks from the Torlesse Supergroup and Waipapa Group in the central North Island, New Zealand: New Zealand Journal of Geology and Geophysics, v. 52, no. 2, p. 149–170, https://doi.org/10.1080/00288300909509883.

Armstrong, P.A., Chapman, D.S., Funnell, R.H., Allis, R.G., and Kamp, P.J., 1996, Thermal modeling and hydrocarbon generation in an active-margin basin: Taranaki Basin, New Zealand: AAPG Bulletin, v. 80, no. 8, p. 1216–1241.

Athy, L.F., 1930, Density, porosity, and compaction of sedimentary rocks: AAPG Bulletin, v. 14, no. 1, p. 1–24.

Ballance, P., 1976, Evolution of the upper Cenozoic magmatic arc and plate boundary in northern New Zealand: Earth and Planetary Science Letters, v. 28, no. 3, p. 356–370, https://doi.org/10.1016/0012-821X(76)90197-7.

Barnes, P.M., and Nicol, A., 2004, Formation of an active thrust triangle zone associated with structural inversion in a subduction setting, eastern New Zealand: Tectonics, v. 23, no. 1, p. •••, https://doi.org/10.1029/2002TC001449.

Beanland, S., Melhuish, A., Nicol, A., and Ravens, J., 1998, Structure and deformational history of the inner forearc region, Hikurangi subduction margin, New Zealand: New Zealand Journal of Geology and Geophysics, v. 41, no. 4, p. 325–342, https://doi.org/10.1080/00288306.1998.9514814.

Begg, M.R., and Johnston, J.G.M., E, 2000, Geology of the Wellington area, scale 1: 250,000 Institute of Geological & Nuclear Sciences Ltd.

Benson, W., 1952, Meeting of the Geological Division of the Pacific Science Congress in New Zealand, February, 1949: Interim Proceedings of the Geological Society of America, v. 1950, p. 11–13.

Berryman, K., Van Dissen, R.J., and Mouslopoulou, V., 2002, Recent rupture of the Tararua section of the Wellington fault and relationships to other fault sections and rupture segments: Institute of Geological & Nuclear Sciences.

Bertaud-Gandar, T.L., Atkins, C.B., and Hannah, M.J., 2018, New stratigraphic constraints on the late Miocene–early Pliocene tectonic development of the Aorangi Range, Wairarapa: New Zealand Journal of Geology and Geophysics, v. 61, no. 1, p. 26–43, https://doi.org/10.1080/00288306.2017.1402791.

Beu, A.G., 1995, Pliocene limestones and their scallops: lithostratigraphy, pectinid biostratigraphy, and paleogeography of eastern North Island late Neogene limestone, Institute of Geological & Nuclear Sciences Limited.

Bland, K. J., and Kamp, P. J., 2006, Geological structure of the forearc basin in central Hawke's Bay, eastern North Island.

Bland, K.J., Kamp, P.J., and Nelson, C.S., 2007, Systematic lithostratigraphy of the Neogene succession exposed in central parts of Hawke's Bay Basin, eastern North Island, New Zealand.

Bland, K.J., Nicol, A., Kamp, P.J., and Nelson, C.S., 2019, Stratigraphic constraints on the late Miocene–Pleistocene evolution of the North Island Fault System and axial ranges in the central Hikurangi subduction margin, New Zealand: New Zealand Journal of Geology and Geophysics, v. 62, no. 2, p. 248–272, https://doi.org/10.1080/00288306.2018.1545675.

Bradshaw, J., Weaver, S., and Muir, R., 1996, Mid-Cretaceous oroclinal bending of New Zealand terranes: New Zealand Journal of Geology and Geophysics, v. 39, no. 3, p. 461–468, https://doi.org/10.1080/00288306.1996.9514726.

Browne, G.H., 1995, Sedimentation patterns during the Neogene in Marlborough, New Zealand: Journal of the Royal Society of New Zealand, v. 25, no. 4, p. 459–483, https://doi.org/10.1080/03014223.1995.9517497.

Browne, G.H., 2004, Late Neogene sedimentation adjacent to the tectonically evolving North Island axial ranges: Insights from Kuripapango, western Hawke's Bay: New Zealand Journal of Geology and Geophysics, v. 47, no. 4, p. 663–674, https://doi.org/10.1080/00288306.2004.9515082.

Burgreen-Chan, B., Meisling, K.E., and Graham, S., 2016, Basin and petroleum system modelling of the East Coast Basin, New Zealand: a test of overpressure scenarios in a convergent margin: Basin Research, v. 28, no. 4, p. 536–567, https://doi.org/10.1111/bre.12121.

Carter, R.t., and Norris, R., 1976, Cainozoic history of southern New Zealand: an accord between geological observations and plate-tectonic predictions: Earth and Planetary Science Letters, v. 31, no. 1, p. 85–94, https://doi.org/10.1016/0012-821X(76)90099-6.

Cashman, S.M., Kelsey, H.M., Erdman, C.F., Cutten, H.N., and Berryman, K.R., 1992, Strain partitioning between structural domains in the forearc of the Hikurangi subduction zone, New Zealand: Tectonics, v. 11, no. 2, p. 242–257, https://doi.org/10.1029/91TC02363.

Chanier, F., and Ferriere, J., 1991, From a passive to an active margin; tectonic and sedimentary processes linked to the birth of an accretionary prism (Hikurangi Margin, New Zealand): Bulletin de la Société Géologique de France, v. 162, no. 4, p. 649–660, https://doi.org/10.2113/gssgfbull.162.4.649.

Chanier, F., and Férriere, J., 1989, On the existance of major tangential movements in the East Coast Range of New Zealand: Their signifcance within the framework of Pacific Plate subduction: Comptes Rendus de L Academie des Sciences, v. 308, no. 18, p. 1645–1650.

Chanier, F., Ferrière, J., and Angelier, J., 1999, Extensional deformation across an active margin, relations with subsidence, uplift, and rotations: The Hikurangi subduction, New Zealand: Tectonics, v. 18, no. 5, p. 862–876, https://doi.org/10.1029/1999TC900028.

Cole, J., 1986, Distribution and tectonic setting of late Cenozoic volcanism in New Zealand: Late cenozoic volcanism in New Zealand, v. 371.

Cole, J., and Lewis, K., 1981, Evolution of the Taupo-Hikurangi subduction system: Tectonophysics, v. 72, no. 1–2, p. 1–21, https://doi.org/10.1016/0040-1951(81)90084-6.

Cooper, R., and Tulloch, A., 1992, Early Palaeozoic terranes in New Zealand and their relationship to the Lachlan Fold Belt: Tectonophysics, v. 214, no. 1–4, p. 129–144, https://doi.org/10.1016/0040-1951(92)90193-A.

Cox, S. C., and Sutherland, R., 2007, Regional geological framework of South Island, New Zealand, and its significance for understanding the active plate boundary: A continental plate boundary: tectonics at South Island, New Zealand, v. 175, p. 19–46.

Crampton, J., Laird, M., Nicol, A., Hollis, C., and Van Dissen, R., Geology at the northern end of the Clarence Valley, Marlborough; a complete record spanning the Rangitata to Kaikoura orogenies, *in* Proceedings Geological Society of New Zealand, New Zealand Geophysical Society 1998 Joint Annual Conference1998, Volume 30.

Crampton, J., Laird, M., Nicol, A., Townsend, D., and Van Dissen, R., 2003, Palinspastic reconstructions of southeastern Marlborough, New Zealand, for mid-Cretaceous-Eocene times: New Zealand Journal of Geology and Geophysics, v. 46, no. 2, p. 153–175, https://doi.org/10.1080/00288306.2003.9515002.

Crampton, J., and Moore, P., 1990, Environment of deposition of the Maungataniwha Sandstone (Late Cretaceous), Te Hoe River area, western Hawke's Bay, New Zealand: New Zealand Journal of Geology and Geophysics, v. 33, no. 2, p. 333–348, https://doi.org/10.1080/00288306.1990.10425691.

Crampton, J.S., 1997, The Cretaceous Stratigraphy of the Southern Hawke's Bay-Wairarapa Region, Institute of Geological & Nuclear Sciences Limited.

Crampton, J.S., Mortimer, N., Bland, K.J., Strogen, D.P., Sagar, M., Hines, B.R., King, P.R., and Seebeck, H., 2019, Cretaceous termination of subduction at the Zealandia margin of Gondwana: The view from the paleo-trench: Gondwana Research, v. 70, p. 222–242, https://doi.org/10.1016/j.gr.2019.01.010.

Cutten, H.N.C., 1988, Stratigraphy of Cretaceous and Tertiary sediments in the vicinity of the Mohaka River, Te Hoe River, Western Hawkes Bay, New Zealand: New Zealand Geological Survey, Department of Scientific and Industrial Research, EDS115, p. 32.

Davy, B., Hoernle, K., and Werner, R., 2008, Hikurangi Plateau: Crustal structure, rifted formation, and Gondwana subduction history: Geochemistry Geophysics Geosystems, v. 9, no. 7, p. •••, https://doi.org/10.1029/2007GC001855.

Delteil, J., Morgans, H.E., Raine, J.I., Field, B.D., and Cutten, H.N., 1996, Early Miocene thin-skinned tectonics and wrench faulting in the Pongaroa district, Hikurangi margin, North Island, New Zealand: New Zealand Journal of Geology and Geophysics, v. 39, no. 2, p. 271–282, https://doi.org/10.1080/00288306.1996.9514711.

Erdman, C.F., and Kelsey, H.M., 1992, Pliocene and Pleistocene stratigraphy and tectonics, Ohara Depression and Wakarara Range, North Island, New Zealand: New Zealand Journal of Geology and Geophysics, v. 35, no. 2, p. 177–192, https://doi.org/10.1080/00288306.1992.9514512.

Field, B., and Uruski, C., 1997, Cretaceous-Cenozoic geology and petroleum systems of the East Coast Region, 301 p.: Inst. of Geol. and Nucl. Sci. Ltd, Lower Hutt, New Zealand.

Forsyth, P., Barrell, D., and Jongens, R., 2008, Geology of the Christchurch area, scale 1: 250000, Institute of Geological & Nuclear Sciences Limited, 1: 250000 Geological Map 16, 1 sheet+ 67 p, Lower Hutt, New Zealand: GNS Science ISBN, p. 67.

Freund, R., 1971, The Hope Fault. A strike slip fault in New Zealand.

Gray, G.G., and Norton, I.O., 1988, A palinspastic Mesozoic plate reconstruction of New Zealand: Tectonophysics, v. 155, no. 1–4, p. 391–399, https://doi.org/10.1016/0040-1951(88)90277-6.

Hall, L.S., Lamb, S.H., and Mac Niocaill, C., 2004, Cenozoic distributed rotational deformation, South Island, New Zealand: Tectonics, v. 23, no. 2, p. •••, https://doi.org/10.1029/2002TC001421.

Hayes, G.P., Furlong, K.P., and Ammon, C.J., 2009, Intraplate deformation adjacent to the Macquarie Ridge south of New Zealand—The tectonic evolution of a complex plate boundary: Tectonophysics, v. 463, no. 1–4, p. 1–14, https://doi.org/10.1016/j.tecto.2008.09.024.

Heron, D.W., 2018, Geological map of New Zealand 1:250,000.: GNS Science, geological map 1. 1 CD.

Holdgate, G., and Grapes, R., 2015, Wairau basin and fault connections across Cook strait, New Zealand: Seismic and geological evidence: Australian Journal of Earth Sciences, v. 62, no. 1, p. 95–121, https://doi.org/10.1080/08120099.2015.986195.

Isaac, M., Moore, P., and Joass, Y., 1991, Tahora Formation: the basal facies of a Late Cretaceous transgressive sequence, northeastern New Zealand: New Zealand Journal of Geology and Geophysics, v. 34, no. 2, p. 227–236, https://doi.org/10.1080/00288306.1991.9514460.

Kamp, P., 1987, Age and origin of the New Zealand orocline in relation to Alpine Fault movement: Journal of the Geological Society, v. 144, no. 4, p. 641–652, https://doi.org/10.1144/gsjgs.144.4.0641.

Kamp, P.J., 1999, Tracking crustal processes by FT thermochronology in a forearc high (Hikurangi margin, New Zealand) involving Cretaceous subduction termination and mid-Cenozoic subduction initiation: Tectonophysics, v. 307, no. 3–4, p. 313–343, https://doi.org/10.1016/S0040-1951(99)00102-X.

Kamp, P.J., Vonk, A.J., Bland, K.J., Hansen, R.J., Hendy, A.J., McIntyre, A.P., Ngatai, M., Cartwright, S.J., Hayton, S., and Nelson, C.S., 2004, Neogene stratigraphic architecture and tectonic evolution of Wanganui, King Country, and eastern Taranaki Basins, New Zealand: New Zealand Journal of Geology and Geophysics, v. 47, no. 4, p. 625–644, https://doi.org/10.1080/00288306.2004.9515080.

Kear, D., 1993, Reflections on major North Island basement rock assemblages and on megafaults: Journal of the Royal Society of New Zealand, v. 23, no. 1, p. 29–41, https://doi.org/10.1080/03036758.1993.10721215.

Kear, D., 2004, Reassessment of Neogene tectonism and volcanism in North Island, New Zealand: New Zealand Journal of Geology and Geophysics, v. 47, no. 3, p. 361–374, https://doi.org/10.1080/00288306.2004.9515062.

Kelsey, H.M., Cashman, S.M., Beanland, S., and Berryman, K.R., 1995, Structural evolution along the inner forearc of the obliquely convergent Hikurangi margin, New Zealand: Tectonics, v. 14, no. 1, p. 1–18, https://doi.org/10.1029/94TC01506.

Kimbrough, D.L., Mattinson, J.M., Coombs, D.S., Landis, C.A., and Johnston, M.R., 1992, Uranium-lead ages from the Dun Mountain ophiolite belt and Brook Street terrane, South Island, New Zealand: Geological Society of America Bulletin, v. 104, no. 4, p. 429–443, https://doi.org/10.1130/0016-7606(1992)104<0429:ULAFTD>2.3.CO;2.

King, P.R., 2000, Tectonic reconstructions of New Zealand: 40 Ma to the present: New Zealand Journal of Geology and Geophysics, v. 43, no. 4, p. 611–638, https://doi.org/10.1080/00288306.2000.9514913.

Kingma, J.T., 1959, The tectonic history of New Zealand: New Zealand Journal of Geology and Geophysics, v. 2, no. 1, p. 1–55, https://doi.org/10.1080/00288306.1959.10431311.

Lamb, S., 1988, Tectonic rotations about vertical axes during the last 4 Ma in part of the New Zealand plate-boundary zone: Journal of Structural Geology, v. 10, no. 8, p. 875–893, https://doi.org/10.1016/0191-8141(88)90101-0.

Lamb, S., 2011, Cenozoic tectonic evolution of the New Zealand plate-boundary zone: A paleomagnetic perspective: Tectonophysics, v. 509, no. 3–4, p. 135–164, https://doi.org/10.1016/j.tecto.2011.06.005.

Lamb, S., and Bibby, H., 1989, The last 25 Ma of rotational deformation in part of the New Zealand plate-boundary zone: Journal of Structural Geology, v. 11, no. 4, p. 473–492, https://doi.org/10.1016/0191-8141(89)90024-2.

Lamb, S., Mortimer, N., Smith, E., and Turner, G., 2016, Focusing of relative plate motion at a continental transform fault: Cenozoic dextral displacement> 700 km on New Zealand's Alpine Fault, reversing> 225 km of Late Cretaceous sinistral motion: Geochemistry Geophysics Geosystems, v. 17, no. 3, p. 1197–1213, https://doi.org/10.1002/2015GC006225.

Lee, J., Bland, K., Townsend, D., and Kamp, P., 2011, Geology of the Hawkes Bay Area, QMAP 1: 250,000 Geological Map: GNS Sciences, Lower Hutt, New Zealand, v. 97.

Leonard, G., Begg, J., Wilson, C., and Leonard, G., 2010, Geology of the Rotorua area, GNS Science, Lower Hutt New Zealand.

Lewis, K., and Pettinga, J., 1993, The emerging, imbricate frontal wedge of the Hikurangi margin. South Pacific sedi-mentary basins: sedimentary basins of the world (ed. by PF Balance): Amsterdam, Elsiever Science Publishers, p. 225–250.

Little, T.A., and Jones, A., 1998, Seven million years of strike-slip and related off-fault deformation, northeastern Marlborough fault system, South Island, New Zealand: Tectonics, v. 17, no. 2, p. 285–302, https://doi.org/10.1029/97TC03148.

Little, T.A., and Mortimer, N., 2001, Rotation of ductile fabrics across the Alpine Fault and Cenozoic bending of the New Zealand orocline: Journal of the Geological Society, v. 158, no. 5, p. 745–756, https://doi.org/10.1144/jgs.158.5.745.

Little, T.A., and Roberts, A.P., 1997, Distribution and mechanism of Neogene to present-day vertical axis rotations, Pacific-Australian plate boundary zone, South Island, New Zealand: Journal of Geophysical Research. Solid Earth, v. 102, no. B9, p. 20,447–20,468, https://doi.org/10.1029/97JB01279.

Mazengarb, C., 1994, Estimating actual displacement along the Alpine Fault; time for a test: Geological Society of New: Zealand Newsletter, v. 105, p. 58.

Mazengarb, C., and Speden, I.G., 2000, Geology of the Raukumara area: Institute of Geological and Nuclear Sciences, Geological Map 6, scale 1:250,000, Lower Hutt, New Zealand.

Mazengarb, C., and Harris, D., 1994, Cretaceous stratigraphic and structural relations of Raukumara Peninsula, New Zealand: stratigraphic patterns associated with the migration of a thrust system, *in* Proceedings Annales Tectonicae, Volume 8, p. 100–118.

Melhuish, A., 1990, Late Cenozoic deformation along the Pacific-Australian plate margin, Dannevirke region, New Zealand: Victoria University of Wellington.

Molnar, P., Atwater, T., Mammerickx, J., and Smith, S.M., 1975, Magnetic anomalies, bathymetry and the tectonic evolution of the South Pacific since the Late Cretaceous: Geophysical Journal International, v. 40, no. 3, p. 383–420, https://doi.org/10.1111/j.1365-246X.1975.tb04139.x.

Moore, P., 1980, Late Cretaceous-Tertiary stratigraphy, structure, and tectonic history of the area between Whareama and Ngahape, eastern Wairarapa, New Zealand: New Zealand Journal of

Geology and Geophysics, v. 23, no. 2, p. 167–177, https://doi.org/10.1080/00288306.1980.10424204.
Moore, P., 1988, Structural divisions of eastern North Island: New Zealand Geological Survey Record, v. 30: Dept. Scientific and Industrial Res., Lower Hutt, p. 19.
Mortimer, N., 1993, Metamorphic zones, terranes, and Cenozoic faults in the Marlborough Schist, New Zealand: New Zealand Journal of Geology and Geophysics, v. 36, no. 3, p. 357–368, https://doi.org/10.1080/00288306.1993.9514581.
[[Not cited?]]Mortimer, N., 1994, Origin of the Torlesse terrane and coeval rocks, North Island, New Zealand: International Geology Review, v. 36, no. 10, p. 891–910, https://doi.org/10.1080/00206819409465494.
Mortimer, N., 2014, The oroclinal bend in the South Island, New Zealand: Journal of Structural Geology, v. 64, p. 32–38, https://doi.org/10.1016/j.jsg.2013.08.011.
Mortimer, N., Campbell, H.J., Tulloch, A.J., King, P.R., Stagpoole, V.M., Wood, R.A., Rattenbury, M.S., Sutherland, R., Adams, C.J., and Collot, J., 2017, Zealandia: Earth's hidden continent: GSA Today, v. 27, no. 3, p. 27–35, https://doi.org/10.1130/GSATG321A.1.
Mumme, T., Lamb, S., and Walcott, R., 1989, The Raukumara paleomagnetic domain: Constraints on the tectonic rotation of the east coast, North Island, New Zealand, from paleomagnetic data: New Zealand Journal of Geology and Geophysics, v. 32, no. 3, p. 317–326, https://doi.org/10.1080/00288306.1989.10425711.
Mumme, T. C., and Walcott, R., 1985, Paleomagnetic studies at geophysics division, 1980–1983: Report-Geophysics Division, no. 204.
Neef, G., 1997, Stratigraphy, structural evolution, and tectonics of the northern part of the Tawhero Basin and adjacent areas, northern Wairarapa, North Island, New Zealand: New Zealand Journal of Geology and Geophysics, v. 40, no. 3, p. 335–358, https://doi.org/10.1080/00288306.1997.9514766.
Nicol, A., Mazengarb, C., Chanier, F., Rait, G., Uruski, C., and Wallace, L., 2007, Tectonic evolution of the active Hikurangi subduction margin, New Zealand, since the Oligocene: Tectonics, v. 26, no. 4, p. •••, https://doi.org/10.1029/2006TC002090.
Nicol, A., and Uruski, C., 2005, Structural Interpretation and Cross Section Balancing, East Coast Basin, New Zealand: Open-File Petroleum Report, Institute of Geological and Nuclear Sciences, Lower Hutt, New Zealand, v. 3184, p. 14.
Nicol, A., VanDissen, R., Vella, P., Alloway, B., and Melhuish, A., 2002, Growth of contractional structures during the last 10 my at the southern end of the emergent Hikurangi forearc basin, New Zealand: New Zealand Journal of Geology and Geophysics, v. 45, no. 3, p. 365–385, https://doi.org/10.1080/00288306.2002.9514979.
Nicol, A., and Wallace, L., 2007, Temporal stability of deformation rates: Comparison of geological and geodetic observations, Hikurangi subduction margin, New Zealand: Earth and Planetary Science Letters, v. 258, no. 3–4, p. 397–413, https://doi.org/10.1016/j.epsl.2007.03.039.
Pondard, N., and Barnes, P.M., 2010, Structure and paleoearthquake records of active submarine faults, Cook Strait, New Zealand: Implications for fault interactions, stress loading, and seismic hazard: Journal of Geophysical Research. Solid Earth, v. 115, no. B12, p. 31.
Pulford, A., and Stern, T., 2004, Pliocene exhumation and landscape evolution of central North Island, New Zealand: the role of the upper mantle: Journal of Geophysical Research. Earth Surface, v. 109, no. F1, p. 12.

Rait, G., Chanier, F., and Waters, D.W., 1991, Landward-and seaward-directed thrusting accompanying the onset of subduction beneath New Zealand: Geology, v. 19, no. 3, p. 230–233, https://doi.org/10.1130/0091-7613(1991)019<0230:LASDTA>2.3.CO;2.
Rattenbury, M.S., Townsend, D.B., Johnston, M.R., compilers, 2006, Geology of the Kaikoura area: Lower Hutt, New Zealand, Institute of Geological and Nuclear Sciences (GNS Science), Geological Map 13, scale 1:250,000, 70 p.
Reilly, C., Nicol, A., Walsh, J.J., and Seebeck, H., 2015, Evolution of faulting and plate boundary deformation in the Southern Taranaki Basin, New Zealand: Tectonophysics, v. 651, p. 1–18, https://doi.org/10.1016/j.tecto.2015.02.009.
Reyners, M., Eberhart-Phillips, D., and Bannister, S., 2011, Tracking repeated subduction of the Hikurangi Plateau beneath New Zealand: Earth and Planetary Science Letters, v. 311, no. 1–2, p. 165–171, https://doi.org/10.1016/j.epsl.2011.09.011.
Reyners, M., Eberhart-Phillips, D., Upton, P., and Gubbins, D., 2017, Three-dimensional imaging of impact of a large igneous province with a subduction zone: Earth and Planetary Science Letters, v. 460, p. 143–151, https://doi.org/10.1016/j.epsl.2016.12.025.
Ridd, M., 1967, Miocene transcurrent movement on the Pongaroa fault, Wairarapa, New Zealand: New Zealand Journal of Geology and Geophysics, v. 10, no. 1, p. 209–216, https://doi.org/10.1080/00288306.1967.10428191.
Rowan, C.J., and Roberts, A.P., 2008, Widespread remagnetizations and a new view of Neogene tectonic rotations within the Australia-Pacific plate boundary zone, New Zealand: Journal of Geophysical Research. Solid Earth, v. 113, no. B3, p. 22.
Schellart, W., Lister, G., and Toy, V., 2006, A Late Cretaceous and Cenozoic reconstruction of the Southwest Pacific region: Tectonics controlled by subduction and slab rollback processes: Earth-Science Reviews, v. 76, no. 3–4, p. 191–233, https://doi.org/10.1016/j.earscirev.2006.01.002.
Sclater, J.G., and Christie, P.A., 1980, Continental stretching: An explanation of the post-mid-Cretaceous subsidence of the central North Sea basin: Journal of Geophysical Research. Solid Earth, v. 85, no. B7, p. 3711–3739, https://doi.org/10.1029/JB085iB07p03711.
Seebeck, H., Nicol, A., Giba, M., Pettinga, J., and Walsh, J., 2014, Geometry of the subducting Pacific plate since 20 Ma, Hikurangi margin, New Zealand: Journal of the Geological Society, v. 171, no. 1, p. 131–143, https://doi.org/10.1144/jgs2012-145.
Silberling, N.J., Nichols, K., Bradshaw, J., and Blome, C., 1988, Limestone and chert in tectonic blocks from the Esk Head subterrane, South Island, New Zealand: Geological Society of America Bulletin, v. 100, no. 8, p. 1213–1223, https://doi.org/10.1130/0016-7606(1988)100<1213:LACITB>2.3.CO;2.
Simandjuntak, T., and Barber, A., 1996, Contrasting tectonic styles in the Neogene orogenic belts of Indonesia: Geological Society of London, Special Publications, v. 106, no. 1, p. 185–201, https://doi.org/10.1144/GSL.SP.1996.106.01.12.
Stagpoole, V., and Nicol, A., 2008, Regional structure and kinematic history of a large subduction back thrust: Taranaki Fault, New Zealand: Journal of Geophysical Research. Solid Earth, v. 113, no. B1, p. 19.
Suggate, R., 1963, The Alpine Fault, *in* Proceedings: Transactions of the Royal Society of New Zealand, v. 2, p. 105–129.
Sutherland, R., 1995, The Australia-Pacific boundary and Cenozoic plate motions in the SW Pacific: Some constraints from Geosat data: Tectonics, v. 14, no. 4, p. 819–831, https://doi.org/10.1029/95TC00930.

Sutherland, R., 1999a, Cenozoic bending of New Zealand basement terranes and Alpine Fault displacement: a brief review: New Zealand Journal of Geology and Geophysics, v. 42, no. 2, p. 295–301, https://doi.org/10.1080/00288306.1999.9514846.

Sutherland, R., 1999b, Basement geology and tectonic development of the greater New Zealand region: an interpretation from regional magnetic data: Tectonophysics, v. 308, no. 3, p. 341–362, https://doi.org/10.1016/S0040-1951(99)00108-0.

Sutherland, R., Davey, F., and Beavan, J., 2000, Plate boundary deformation in South Island, New Zealand, is related to inherited lithospheric structure: Earth and Planetary Science Letters, v. 177, no. 3–4, p. 141–151, https://doi.org/10.1016/S0012-821X(00)00043-1.

Trewick, S., and Bland, K., 2012, Fire and slice: palaeogeography for biogeography at New Zealand's North Island/South Island juncture: Journal of the Royal Society of New Zealand, v. 42, no. 3, p. 153–183, https://doi.org/10.1080/03036758.2010.549493.

Uruski, C., 1992, Sedimentary basins & structure of Cook Strait, Institute of Geological and Nuclear Sciences Limited, Lower Hutt, New Zealand.

Uruski, C., and Wood, R., 1993, The Hikurangi Triangle and its effect on the petroleum geology of the East Coast Basin: Pet. Expl. NZ News, Wellington, New Zealand, p. 8–17.

van der Meer, Q.H., Storey, M., Scott, J.M., and Waight, T.E., 2016, Abrupt spatial and geochemical changes in lamprophyre magmatism related to Gondwana fragmentation prior, during and after opening of the Tasman Sea: Gondwana Research, v. 36, p. 142–156, https://doi.org/10.1016/j.gr.2016.04.004.

Van Dissen, R., and Yeats, R.S., 1991, Hope fault, Jordan thrust, and uplift of the seaward Kaikoura Range, New Zealand: Geology, v. 19, no. 4, p. 393–396, https://doi.org/10.1130/0091-7613(1991)019<0393:HFJTAU>2.3.CO;2.

Van Dissen, R.J., 1989, Late Quaternary faulting in the Kaikoura region, southeastern Marlborough, New Zealand [M.S. thesis]: Corvallis, Oregon, Oregon State University.

Vickery, S., and Lamb, S., 1995, Large tectonic rotations since the Early Miocene in a convergent plate-boundary zone, South Island, New Zealand: Earth and Planetary Science Letters, v. 136, no. 1–2, p. 43–59, https://doi.org/10.1016/0012-821X(95)00140-3.

Walcott, R., 1984, Reconstructions of the New Zealand region for the Neogene: Palaeogeography, Palaeoclimatology, Palaeoecology, v. 46, no. 1–3, p. 217–231, https://doi.org/10.1016/0031-0182(84)90035-X.

Walcott, R., 1998, Modes of oblique compression: Late Cenozoic tectonics of the South Island of New Zealand: Reviews of Geophysics, v. 36, no. 1, p. 1–26, https://doi.org/10.1029/97RG03084.

Walcott, R., Christoffel, D., and Mumme, T., 1981, Bending within the axial tectonic belt of New Zealand in the last 9 Myr from paleomagnetic data: Earth and Planetary Science Letters, v. 52, no. 2, p. 427–434, https://doi.org/10.1016/0012-821X(81)90195-3.

Wallace, L., Barnes, P., Beavan, J., Van Dissen, R., Litchfield, N., Mountjoy, J., Langridge, R., Lamarche, G., and Pondard, N., 2012, The kinematics of a transition from subduction to strike-slip: An example from the central New Zealand plate boundary: Journal of Geophysical Research. Solid Earth, v. 117, no. B2, p. 24.

Wallace, L.M., Beavan, J., McCaffrey, R., Berryman, K., and Denys, P., 2007, Balancing the plate motion budget in the South Island, New Zealand using GPS, geological and seismological data: Geophysical Journal International, v. 168, no. 1, p. 332–352, https://doi.org/10.1111/j.1365-246X.2006.03183.x.

Wallace, L.M., Beavan, J., McCaffrey, R., and Darby, D., 2004, Subduction zone coupling and tectonic block rotations in the North Island, New Zealand: Journal of Geophysical Research. Solid Earth, v. 109, no. B12, p. 21.

Wellman, H., 1956, Structural outline of New Zealand, Department of Scientific and Industrial Research, Lower Hutt, New Zealand, v. 121.

Wellman, H.W., 1971, Age of the Alpine Fault, New Zealand.: Proceedings of the 22nd International Geological Congress no. 4, p. 148–162.

Wells, P.E., 1989, Late Neogene stratigraphy of the Carrington area, western Wairarapa, North Island, New Zealand: Journal of the Royal Society of New Zealand, v. 19, no. 3, p. 283–303, https://doi.org/10.1080/03036758.1989.10427183.

Wood, R., and Stagpoole, V., 2007, Validation of tectonic reconstructions by crustal volume balance: New Zealand through the Cenozoic: Geological Society of America Bulletin, v. 119, no. 7–8, p. 933–943, https://doi.org/10.1130/B26018.1.

Table S1: Additional declination anomaly data from various localities around New Zealand, not included in the Lamb (2011) paleomagnetic data compilation.

Locality	Domain	Declination Anomaly	Age (Ma)	Reference
Dun Mountain	Australian	25	280 (±5)	Hunt & Smith (1980)
South Auckland	Australian	6.3	1 (±0.5)	Briggs *et al.* (1994)
Northland	Australian	60.9	160	Haston & Luyendyk (1991)
Northland Ophiolite	Australian	-17.8	27.5 (±1.5)	Cassidy (1993)
Matakaoa	East Coast	7	90 (±5)	Hunt & Smith (1980)
Kopua	East Coast	22.3	5.5 (±0.5)	Fujii *et al.* (1994)
Kopua	East Coast	23.5	1.6 (±0.3)	Fujii *et al.* (1994)
Horerua	East Coast	27	6 (±0.5)	Fujii *et al.* (1994)
Muanga Rd	East Coast	13.5	4 (±0.5)	Fujii *et al.* (1994)
Muanga Rd	East Coast	40	1.6 (±0.3)	Fujii *et al.* (1994)
Rangitato	East Coast	69	60 (±5)	Fujii *et al.* (1994)
Manawatu River	East Coast	9.9	1.6 (±0.3)	Fujii *et al.* (1994)
Blue Mountain	Marlborough	25	95 (±5)	Hunt & Smith (1980)
Mead Stream	Marlborough	56.7	50 (±5)	Dallanave *et al.* (2015)
Swampy Summit	Pacific	-22.3	12.4	Sherwood (1988)
Dunedin Volcano	Pacific	4	11.75 (±1.25)	Sherwood (1988)
Lytlleton volcano	Pacific	1.9	11 (±1.2)	Sherwood (1988)
Akaroa Volacano	Pacific	23	9 (±0.5)	Sherwood (1988)
Mt Somers	Pacific	-6	95 (±2)	Oliver *et al.* (1979)
mid-Waipara River	Pacific	41.5	50 (±5)	Dallanave *et al.* (2016)
Mt Somers	Pacific	9	95 (±2)	Hunt & Smith (1980)
Mt Somers	Pacific	15	95 (±2)	Hunt & Smith (1980)
Banks Penisula	Pacific	11	10 (±0.7)	Hunt & Smith (1980)
Otago Penisula	Pacific	10	11 (±1)	Hunt & Smith (1980)
Otago Penisula	Pacific	5	11 (±1)	Hunt & Smith (1980)
Chathams	Pacific	3	4 (±0.5)	Hunt & Smith (1980)
Chathams	Pacific	11	45 (±5)	Hunt & Smith (1980)
Takitimu	Pacific	-83.2	190 (±10)	Haston *et al.* (1989)
White Hill	Pacific	56.4	190 (±10)	Haston *et al.* (1989)
Takitimu average	Pacific	-13	190 (±10)	Haston *et al.* (1989)
Chatham Islands	Pacific	-5.7	5 (±1)	Grindley *et al.* (1977)
Chatham Islands	Pacific	14.2	34 (±8)	Grindley *et al.* (1977)
Chatham Islands	Pacific	-5.5	90 (±8)	Grindley *et al.* (1977)
TVZ	TVZ	19	0.5 (±0.2)	Hunt & Smith (1980)
TVZ	TVZ	11	0.5 (±0.2)	Hunt & Smith (1980)
Rangipo Headrace	TVZ	1	0.5 (±0.2)	Hunt & Smith (1980)
Waiotapu	TVZ	-1.9	0.6 (±0.3)	Grindley *et al.* (1994)
Maroa	TVZ	4.4	0.2 (±0.05)	Tanaka *et al.* (1996)

Table S2: Average strike orientation of basement and mid-Cretaceous strata in the North Island East Coast Basin. Strike and dip data extracted from QMAP 1:250,000 sheets (Begg & Johnston, 2000; Mazengarb & Speden, 2000; Lee & Begg, 2002; Lee *et al.*, 2011). Standard deviation (σ), number of observations (n).

Locality	Unit	Basement / Cover	Mean Strike	σ	n	Percent within X° of Vertical		Region	Deviation from Mean Northland Strike Trend (Degrees Clockwise)
						25°	45°		
Rimutaka Range	Esk Head Belt	Basement	202	31	43	67	93	Wellington	54
Aorangi Mountains	Pahau Terrane (undiff.)	Basement	195	34	36	78	100	Wellington	47
Tora-Glenburn	Pahaoa Group	Basement	198	32	24	42	96	Wellington	50
Owahanga	Pahaoa Group	Basement	198	27	12	83	100	Wairarapa	50
Ngahape area	Pahaoa Group	Basement	199	32	11	0	27	Wairarapa	51
Tinui area	Pahaoa Group	Basement	201	33	46	48	85	Wairarapa	53
Waewaepa Range	Waioeka petrofacies	Basement	205	41	3	100	100	Wairarapa	57
Axial Ranges	Esk Head Belt	Basement	225	22	7	71	100	Hawke's Bay	77
Wakarara Range	Waioeka petrofacies	Basement	196	43	8	63	88	Hawke's Bay	48
East Ruahine foothills	Waioeka petrofacies	Basement	200	33	33	52	82	Hawke's Bay	52
West Raukumara Range	Waioeka petrofacies	Basement	181	42	57	46	89	Raukumara	33
Central Raukumara Range	Pahau Terrane (undiff.)	Basement	196	56	12	42	75	Raukumara	48
East Raukumara Range	Omaio petrofacies	Basement	192	50	73	56	82	Raukumara	44
Mt Hikurangi area	Waitahaia Formation	Basal Cover Sequence	175	39	104	41	66	Raukumara	27
Mangaotane Stream area	Base Karekare Formation	Basal Cover Sequence	183	62	60	25	50	Raukumara	35
Tapuaeroa-Waikura River area	Mokoiwi Formation	Basal Cover Sequence	169	63	41	22	51	East Coast Allochthon	21
Waitahia-Mata River area	Mokoiwi Formation	Basal Cover Sequence	173	65	13	15	31	East Coast Allochthon	25
Cape Runaway	Matakaoa Volcanics	Basal Cover Sequence	155	66	13	38	69	East Coast Allochthon	7